water

MDPI

Article

Optimization of LID Strategies for Urban CSO Reduction and Cost Efficiency: A Beijing Case Study

Hao Wang [1], Pengfei Zeng [1], Zilong Liu [2], Wentao Li [1,3] and Jinjun Zhou [1,*]

1 Faculty of Architecture, Civil and Transportation Engineering, Beijing University of Technology, Beijing 100124, China
2 Beijing Municipal Institute of City Planning and Design, Beijing 100045, China
3 Guangzhou Municipal Engineering Design & Research Institute Co., Ltd., Guangzhou 510095, China
* Correspondence: zhoujj@bjut.edu.cn

Abstract: Combined sewer overflow (CSO) can lead to serious urban water environment pollution and health risks to residents. Low Impact Development (LID) facilities are one of the important measures to alleviate CSO and have been widely applied. The rational selection of LID facility types, locations, and scales is the most important task, which can effectively improve resource utilization efficiency. Based on the NSGA-II multi-objective optimization algorithm and coupled with the SWMM sewer network hydraulic model, this study takes the combined sewer overflows and the construction cost of LID facilities as optimization objectives and optimizes the types and scales of LID layout in the study area, including eight different return periods. By using the Pareto frontier and visualizing the results of the model, the effects of different rainfall return periods on the CSO control and investment cost of LID layout schemes are compared. The results show the following: (1) the optimization model can demonstrate the relationship between CSO control volume and LID construction cost under different LID layout schemes through the Pareto frontier, showing three different trends, indicating that the relationship between overflow volume and investment cost is nonlinear; (2) with the increase in rainfall intensity, higher requirements are proposed for LID schemes to meet CSO control targets, leading to a decrease in the number of Pareto frontier solution sets. Under larger rainfall intensities, it is difficult to achieve the same overflow control effect by increasing the scale of LID construction. Therefore, considering constraining the LID construction cost between RMB 5.3 and 5.38 million is helpful to determine the most suitable solution; (3) in the optimal layout schemes under different return periods, 87.3% of the locations where LID is deployed have similar scales. Based on these locations with a relatively large proportion of deployment, it can be determined that special attention should be paid to spatial positions in LID planning and construction. This study provides valuable insights for solving combined sewer overflow problems and optimizing urban drainage management and provides guidance for future planning and decision-making processes.

Keywords: SWMM; combined sewer overflows; low impact development; NSGA-II

Citation: Wang, H.; Zeng, P.; Liu, Z.; Li, W.; Zhou, J. Optimization of LID Strategies for Urban CSO Reduction and Cost Efficiency: A Beijing Case Study. *Water* **2024**, *16*, 965. https://doi.org/10.3390/w16070965

Academic Editor: Craig Allan

Received: 28 February 2024
Revised: 19 March 2024
Accepted: 25 March 2024
Published: 27 March 2024

1. Introduction

The combined sewer overflow refers to the direct discharge of untreated rainwater runoff into water bodies when rainfall runoff exceeds the capacity of the drainage system, leading to pollution [1]. CSO is a common cause of urban water body pollution, primarily due to the lag in the development of drainage systems compared to urban expansion [2]. In recent years, significant changes in urban land cover have increased the frequency of CSO [3]. However, improving the interception factor through sewer network reconstruction to alleviate CSO is challenging due to constraints such as infrastructure complexity, land limitations, engineering difficulties, and social impacts [4]. In this context, Green Infrastructure/Low Impact Development has gained widespread attention as a surface runoff control method [5,6]. LID, as a rainwater management concept, aims to minimize the environmental impact of land development and maintain rainwater runoff at levels resembling natural conditions [7].

LID facilities, including permeable pavement, green roofs, and rain gardens, play a significant role in reducing surface impervious rate and enhancing rainwater retention, infiltration, and reuse. By decreasing the volume of runoff entering drainage systems, LID facilities can mitigate urban flooding disasters [8], optimize rainwater resource utilization [9], and mitigate CSO pollution [10]. Previous research by numerous researchers and experts has extensively explored and applied LID facilities. Liu et al. [11] devised a comprehensive evaluation methodology and investigated the runoff control efficacy of various LID facility types. Studies conducted by Gao and Zeng et al. [12,13] have yielded valuable insights into integrating different LID facilities to address urban flooding scenarios. Additionally, Liao et al. [14] explored strategies that integrate LID with traditional sewer network refurbishment to minimize the frequency and impact of CSO incidents. These studies furnish crucial theoretical underpinnings and practical directives for comprehending and implementing LID in managing rainwater and CSO challenges.

In the deployment of LID facilities, optimizing their placement is important. This optimization can improve resource utilization efficiency, mitigate surface waterlogging issues, alleviate network loads, and comprehensively address multiple objectives, thereby offering scientific decision support for policymakers. Yao et al. [15] investigated the planning and design strategies for the spatial location of green roofs in urban catchment areas to minimize runoff and peak flow. Tansar et al. [16] examined the spatial-scale impact of LID facilities on flood prevention across various rainfall scenarios by strategically siting them upstream, midstream, and downstream within a region. Cheng et al. [17] analyzed the arrangement of LID facilities focusing on three control objectives: runoff control, flood control, and waterlogging mitigation. Integrating hydrological modeling with multi-objective optimization methods is recognized as an effective approach to maximizing the performance of LID facilities under constrained conditions. In a related study, Saniei et al. [18] optimized the size, type, and location of LID in urban watersheds by integrating the SWMM with the NSGA-II algorithm, taking into account long-term rainfall conditions in the urban watershed. Ambrogi et al. [19] coupled NSGA-II with the SWMM to determine the optimal locations for bioretention cells, green roofs, and permeable pavements, aiming to maximize infiltration with LID at the lowest cost in a small urban watershed. Similarly, Yu et al. [20] utilized NSGA-II, developing an SWMM- and MATLAB-based method for LID deployment planning, with findings indicating the efficacy of multi-objective optimization in reducing runoff. These studies on LID layout optimization all utilized runoff volume, runoff depth, and peak flow as control objectives. However, using surface runoff indicators as control metrics for LID facilities may not fully optimize performance during the overflow process in detention basins within the network system.

To solve the above problems, this study couples NSGA-II with SWMM to construct a multi-objective optimization model. Considering the reduction in LID construction and operation costs, as well as the overload status of weirs in combined sewer systems, the optimal combination and scale of LID types are determined. Using the optimization model, simulations are conducted under different rainfall scenarios to compare the differences in LID deployment optimization results under various design storms. Based on the simulation results, decisions regarding LID design choices are made, and critical LID deployment locations are identified to provide rational construction recommendations.

2. Materials and Methods

Figure 1 illustrates the technical route of this study. Initially, data concerning the drainage network and land cover within the research area, along with design rainfall data for different return periods, are collected. Subsequently, the SWMM software (version 5.2) is utilized to construct the hydraulic model of the drainage network in the study area, followed by calibration and validation processes. Next, parameters for LID facilities are generalized and configured. On the Python (version 3.10) platform, the SWMM model is coupled with the NSGA-II multi-objective optimization model, with the types and areas of LID facilities in each sub-catchment as optimization variables. Through simulation, optimized deployment schemes for LID under different return periods, as well as the effectiveness of CSO control and LID construction costs, are obtained and analyzed, highlighting disparities in optimal LID deployment schemes under different return period rainfall events.

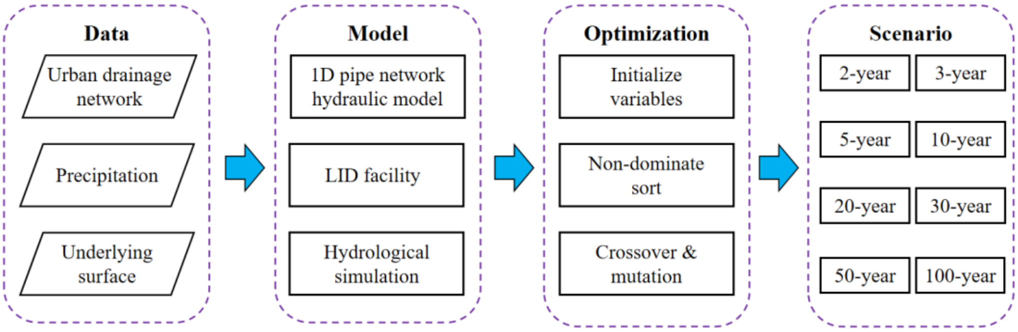

Figure 1. Flowchart of the modeling framework used in this study.

2.1. Study Area

The study area is located in the core functional area of Beijing, the capital of China (39°54′ N, 116°25′ E), which is an important center for the country's political and cultural activities as well as international exchanges. The region is in a warm, semi-humid continental climate zone, with an average annual precipitation of about 698.4 mm, 80% of which occurs during the rainy season (June to September). As shown in Figure 2, the drainage area of the research area is approximately 3.27 square kilometers, mainly comprising residential land, public facilities land, commercial land, and green space, with impermeable surfaces predominating. To the west, there is a channel flowing from north to south, turning east at its southernmost point. The interception main pipe is laid along this channel. This area belongs to the old city area, with outdated living environment facilities and inadequate infrastructure. The construction standards of the drainage system are outdated, leading to frequent overflow of the pipe network and a higher pollution load from rainwater discharge. To address the problem of CSO, it is recommended to design and implement LID measures within the research area.

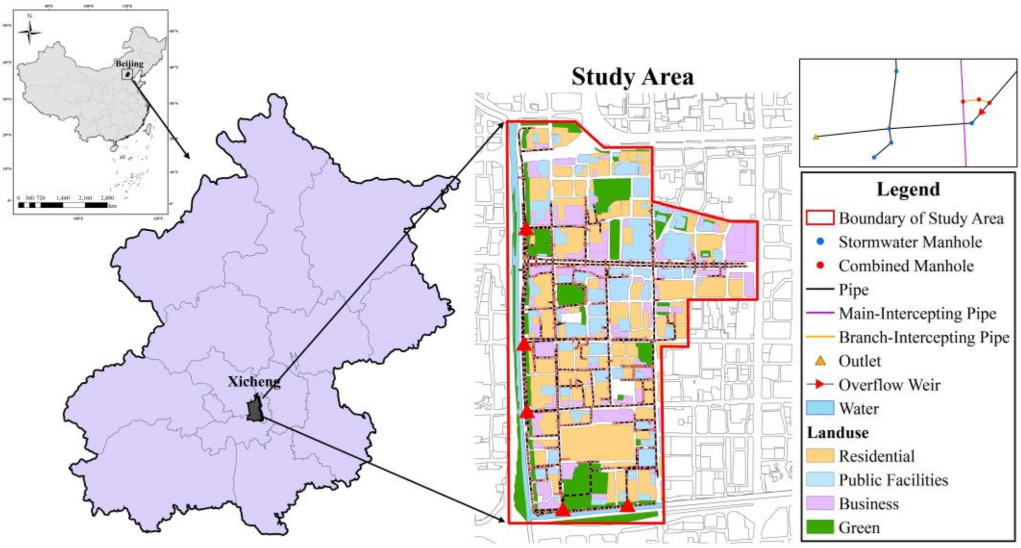

Figure 2. Overview of the urban drainage area.

2.2. Design Storms

The study aims to assess the effectiveness of LID facilities in mitigating CSO incidents during rainstorm events of varying return periods. The design rainfall utilized in this analysis follows the formula outlined in the Beijing local standard [21]. The equation for rainstorm intensity is presented as follows (Equation (1)):

$$q = \frac{A + C\ln P}{(t+B)^n} = \frac{12.126 + 15.012\ln P}{(t+13.8)^{0.748}} \quad (1)$$

where q is the designed rainstorm intensity (mm/min); t is the rainfall duration (min); P is the return period (year); n is the attenuation coefficient of the rainstorm; and A, B and C are regional parameters, the values are calculated as 12.126, 15.012 and 13.8.

Figure 3 illustrates the design rainfall patterns and depths for duration spanning eight return periods.

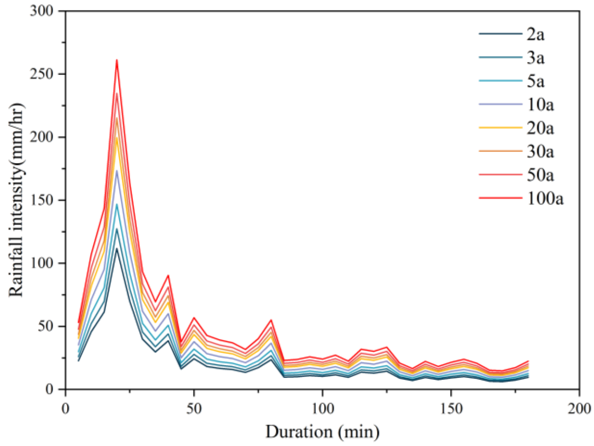

Figure 3. Design rainfall for eight different return periods in Beijing.

2.3. Storm Water Management Model

2.3.1. Construction of SWMM Model

The study employs the Storm Water Management Model (SWMM) developed by the United States Environmental Protection Agency (version 5.2) to simulate the hydrological processes in the study area. It investigates the combined sewer overflow behavior in the sewer network under various LID deployment schemes. Based on data provided by the local drainage management department, a SWMM model of the study area's sewer network was constructed, as shown in Figure 4a. The total length of the sewer network is 32.9 km, comprising 1615 nodes (including 489 rainwater nodes, 625 combined sewer nodes, and 501 sewage nodes), 1620 pipe segments, 5 interceptor weirs, and 8 drainage outlets. Additionally, the study area is equipped with 2 flow meters on the sewage network and 2 liquid level monitors on the rainwater network.

The combined sewer system requires considerations for model construction and parameter settings for both the stormwater and wastewater models. Initially, the study area was divided into 1114 stormwater sub-catchments using the Thiessen polygon method [22]. The Horton model was selected to calculate infiltration. This model is suitable for urban areas based on the description of infiltration mechanisms in SWMM and the characteristics of the underlying surface of the study area. Land use data for the study area includes roads, buildings, green spaces, and water systems. Based on these land use data (Figure 4b), runoff and routing parameters were determined for each sub-catchment. Empirical values for the composite runoff coefficients corresponding to different levels of urban land distribution according to regional planning and design [23] are provided in Table 1.

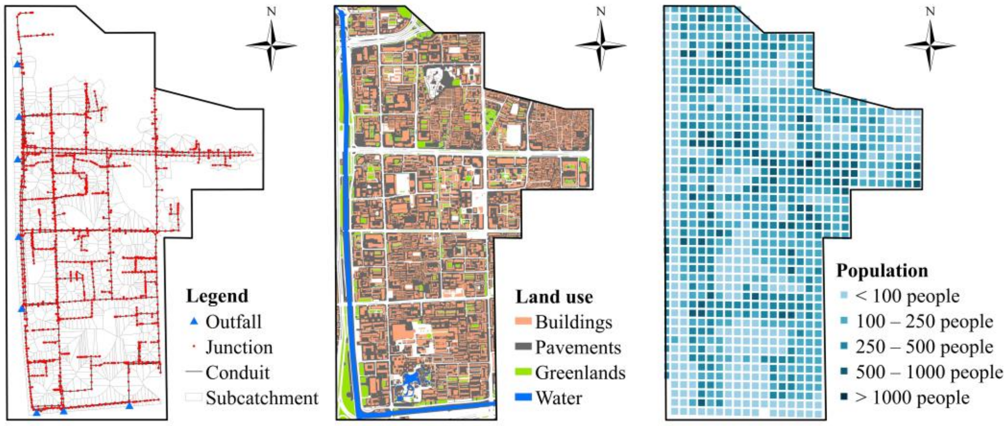

(a) (b) (c)

Figure 4. (**a**) Schematic diagram of the SWMM model; (**b**) land use distribution; and (**c**) population distribution.

Table 1. Empirical values of urban comprehensive runoff coefficient.

Urban Area Situation	Comprehensive Runoff Coefficient
Central areas with densest buildings (impervious area ratio > 70%)	0.6–0.8
Residential areas with denser buildings (50% < impervious area ratio < 70%)	0.5–0.7
Residential areas with sparser buildings (30% < impervious area ratio < 50%)	0.4–0.6
Residential areas with sparsest buildings (impervious area ratio < 30%)	0.3–0.5

The discharge of domestic sewage requires accounting for temporal variations in drainage. Based on daily flow monitoring data from August 2021 to July 2022, statistical methods were employed to derive variation curves for node flow. The distributional quality of the fitted flow data was described using the empirical distribution function-type Kolmogorov–Smirnov test and the Anderson–Darling statistic [24]. The time-varying curves of nodal inflow are acquired by linking the expectation of the probability density distribution function at each moment [25]. In the SWMM model, the discharge of domestic sewage was generalized as nodal inflow of manholes. The manhole receiving the nodal inflow is the receiving sewage manhole in the upstream pipe section of each sewage flow monitoring device. Drainage quotas were allocated to each sewage node based on sub-watershed area and population density data, and sewage discharge simulations were completed by combining the inferred temporal variation curves of the nodes. This approach results in four sewage model curves for the study area, which are depicted in Figure 5.

2.3.2. Calibration and Verification of Model

The calibration of the model for dry conditions was performed using flow data collected from sewage pipelines, while calibration for rainy conditions utilized liquid level data from rainwater pipelines. For both dry and rainy scenarios, one calibration and one validation scenario were selected. The Nash Efficiency Coefficient (NSE) was computed to assess the agreement between model simulations and actual monitoring values [18]. The calibration and validation processes for the sewage flow yielded NSE coefficients of 0.88, 0.78, 0.72, and 0.73, while those for the rainwater level processes resulted in NSE coefficients of 0.72, 0.74, 0.83, and 0.9, as illustrated in Figure 6. Thus, the model meets the required standards and can be applied to simulate combined sewer overflows under different rainy scenarios.

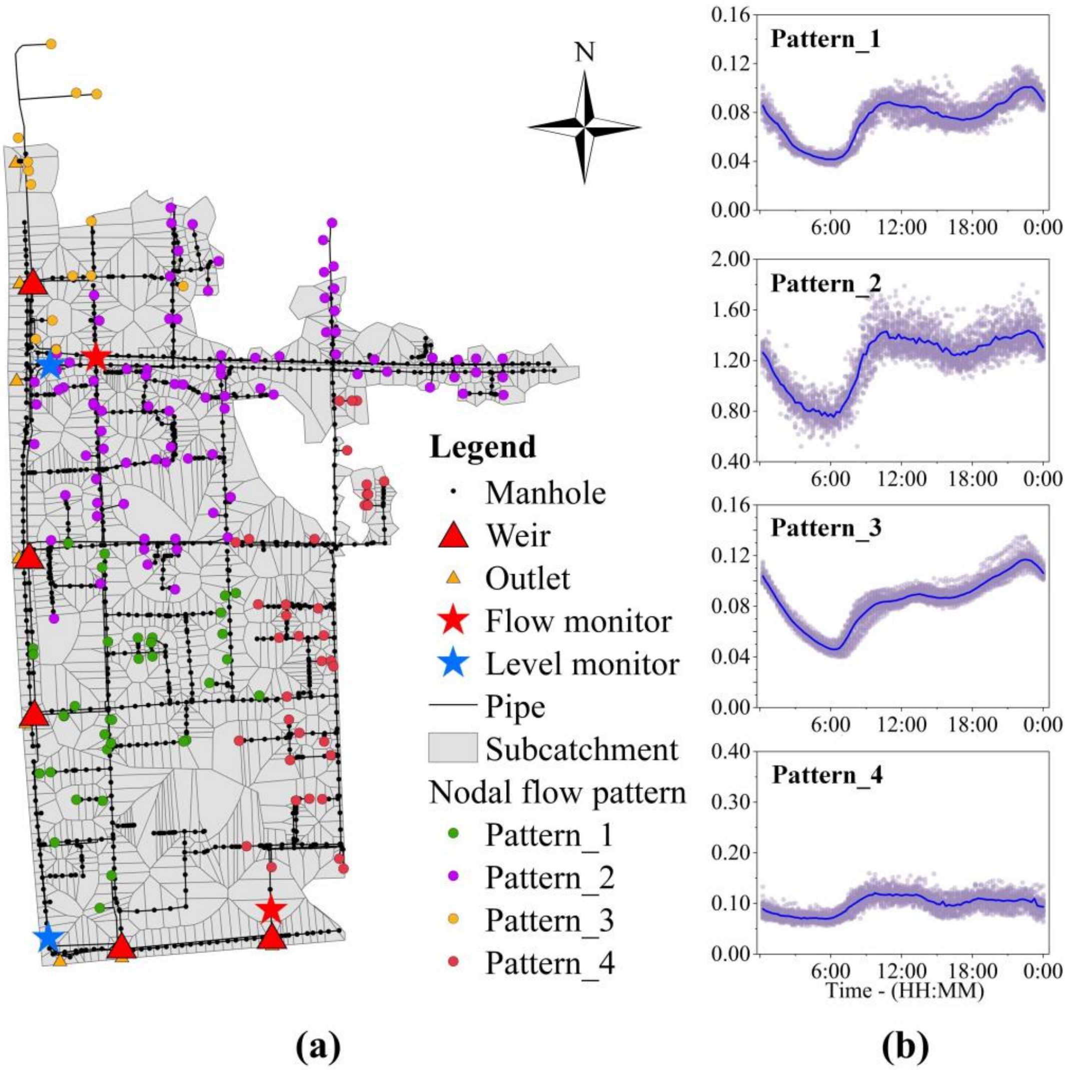

Figure 5. (**a**) Hydraulic model of drainage network in the study area and (**b**) nodal flow diurnal patterns.

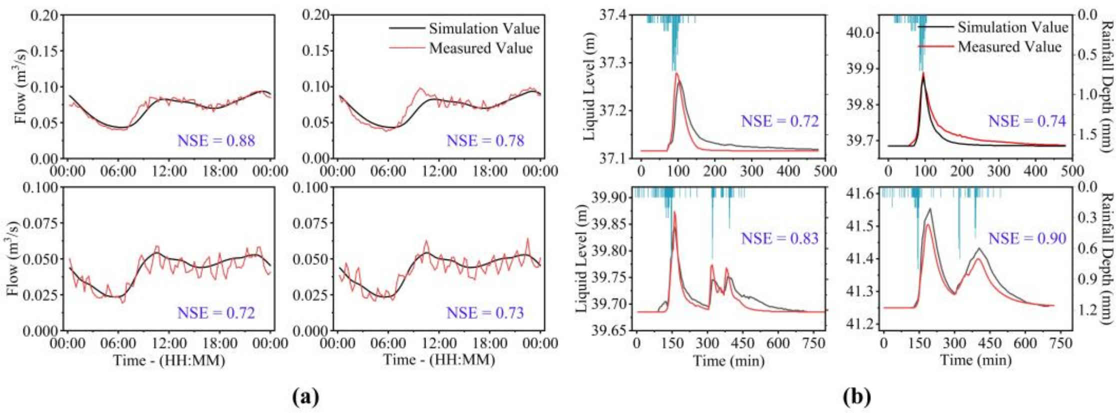

Figure 6. Measured and simulated process lines for calibration and validation (**a**) dry model; and (**b**) storm model.

2.3.3. LID Facilities Setting

Based on the drainage system planning and urban sponge city construction design standards in Beijing, three LID measures were designed for the study area, including permeable pavement, green roofs, and rain gardens [26]. As shown in Figure 4b, permeable pavement is built on pavement surfaces, green roofs are distributed on buildings, and rain gardens are installed on greens. Parameters for the three LID facilities were set based on the relevant literature and empirical values [17], as presented in Table 2.

Table 2. LID facility parameter settings.

Process	Parameter	Permeable Pavement	Green Roof	Rain Garden
Surface layer	Berm Height/mm	0.00	80.00	200.00
	Vegetation Volume	0.00	0.20	0.20
	Surface Roughness	0.10	0.10	0.60
	Surface Slope/%	0.20	0.50	5.00
Soil layer	Porosity	0.50	0.50	0.50
	Wilting Point	0.10	0.085	0.05
	Field Capacity	0.20	0.20	0.10
	Thickness/mm	150.00	150.00	700.00
	Suction Head/mm	100.00	100.00	100.00
	Conductivity Slope	30.00	30.00	30.00
	Conductivity/(mm/h)	150.00	100.00	200.00
Storage layer	Void Ratio	0.75	-	0.75
	Thickness/mm	200.00	-	0.00
	Clogging Factor	0.00	-	0.00
	Seepage Rate/(mm/h)	12.50	-	0.50

2.4. Optimization Model

The optimization model couples SWMM with optimization algorithms to optimize the design of LID schemes. A bi-objective optimization model was proposed considering the CSO status of the drainage system and the cost of implementing LID measures. To ensure the model's applicability to the study area, the optimal variables were simulated and encoded based on the measured areas of different land cover types within each sub-basin. Python was chosen as the development platform for the model.

2.4.1. Objective Functions

The first objective function of the optimization model considers the total overflow volume from all interceptor weirs in the study area. The aim is to minimize the total overflow volume by selecting the design scheme with the least overflow, thus achieving optimal pollution control performance. After SWMM simulation, the overflow processes for each interceptor weir can be extracted from the ".rpt" file generated by SWMM operation results.

$$\text{Min } V_{of} = \sum_1^n \sum_1^T Q_t \quad (2)$$

where V_{of} is the total volume of CSO; Q_t is the overflow flow rate of interceptor weir at t time; T is total simulation time; and n is number of interceptor weirs.

The other objective function considers the investment cost of LID construction, aiming to minimize the cost of LID deployment. This objective is utilized to control the budget of the schemes, achieving higher cost-effectiveness. By attaining better benefits with the lowest investment cost, the optimization goal is achieved.

$$\min C = \sum_1^n C_{pp} \times S_{pp} + C_{gr} \times S_{gr} + C_{rg} \times S_{rg} \quad (3)$$

where C is the total investments of LID facilities; S_{pp}, S_{gr}, S_{rg} are the areas of permeable pavement, green roofs, and rain garden; C_{pp}, C_{gr}, C_{rg} are the unit construction costs for permeable pavement, green roofs, and rain gardens. These costs can be referenced from the unit costs of LID facilities as outlined in the "Sponge City Construction Technical Guide" [27] specifically in Table 3.

Table 3. LID facility cost.

LID Facility	Unit Infrastructure Cost ($RMB \cdot m^{-2}$)	Unit Maintenance Cost ($RMB \cdot m^{-2} \cdot a^{-1}$)
Permeable Pavement	200	8.70
Green Roof	300	6.00
Rain Garden	800	55.00

2.4.2. Optimal Variables

The objective of optimizing the model is to determine the layout scheme of Low Impact Development facilities in the study area, requiring the identification of the types and scales of LID facilities in each sub-catchment. Therefore, the optimization variables are the deployment areas of the three types of LID facilities in each sub-catchment. Based on the principles of deployment of LID measures in the study area outlined in Section 2.3.3 and underlying surface data, the possible distribution points and maximum areas for the three types of LID facility have been determined, as shown in Figure 7. Using their maximum areas as upper limits and 0 as lower limits, they serve as constraints for each optimization variable.

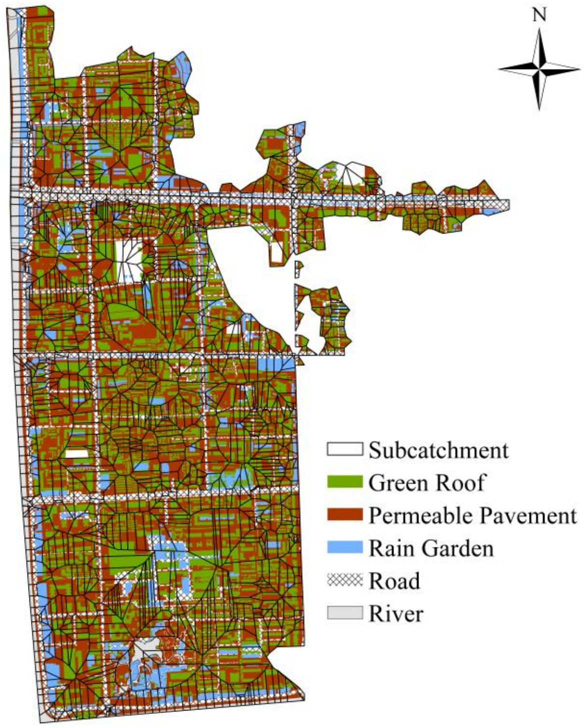

Figure 7. Distribution of different types of LID facilities.

2.4.3. Linkage of NSGA-II to the SWMM model

NSGA-II is widely used in multi-objective optimization of LID measures, and is capable of generating optimal or near-optimal solutions to balance the relationships between competing objectives. NSGA-II is developed based on the Non-dominated Sorting Genetic Algorithm (NSGA). After generating offspring populations through crossover and mutation, the offspring populations are merged with the parent population, and optimal competition is conducted to ensure that the best individuals in the parent population are not destroyed or lost. During the iterative computation process, SWMM is used to simulate CSO processes under LID deployment and to solve the objective functions. Before conducting optimization calculations, it is necessary to establish an SWMM model for the study area and then integrate the optimization algorithm with the simulation of the SWMM model for iterative computation. The steps of the optimization model are summarized as follows, as shown in Figure 8.

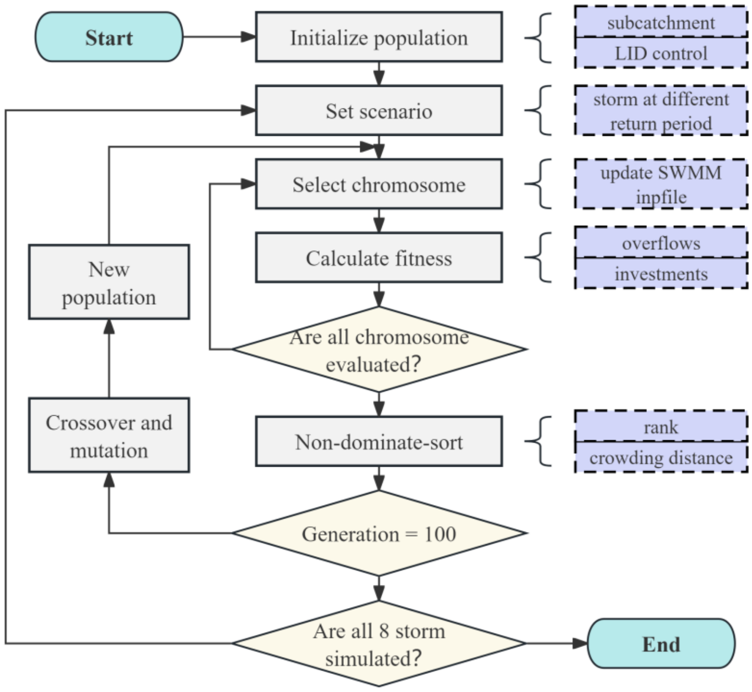

Figure 8. The optimal procedure of the optimization model.

Step 1: Construct an SWMM model for optimizing LID layout: based on the network of pipes and their ancillary facilities, rainfall data, and generalized types and parameter settings of LID facilities, construct an SWMM model for the study area, and use this model to solve the objective function during the iterative process.

Step 2: Initialize the population: Determine the upper and lower limits of the optimization variables based on the size and types of underlying surface data in the study area, and randomly generate the LID deployment conditions within each catchment area. Each population consists of 100 individuals, with each individual containing information on the deployment areas of the three types of LID facilities in all sub-catchment areas.

Step 3: Calculate fitness: Use file reading and PYSWMM in Python to write the population information of generated LID areas into the ".inp" file's sub-catchment and LID_USAGE fields. Then, load the SWMM dynamic link library, conduct hydrological process simulation and result reading, and use the total overflow from weirs as the first objective function value. Calculate the total investment cost based on the LID deployment scheme as the second objective function value.

Step 4: Non-dominated sorting: Perform non-dominated sorting of the population based on fitness. Between two individuals, the one with smaller values for both objective functions has dominance. Based on the non-dominance relationship between individuals, divide them into different ranks, where individuals with higher ranks are considered superior LID solutions.

Step 5: Crowding distance calculation: Within each rank, calculate the crowding distance between individuals based on the difference in overflow and cost. The crowding distance indicates the density around an individual and is used to maintain population diversity.

Step 6: Select the next generation: During crossover, randomly recombine the LID facilities within each sub-catchment of two parent individuals to generate two offspring individuals. Mutation operations initialize the LID area in random sub-catchments of individuals. Select individuals from the current population for crossover and mutation operations to generate a new population.

Step 7: Repeat steps 2 to 6 until the specified number of iterations is reached.

The model outputs a Pareto frontier to obtain the optimal solution in the form of a two-dimensional curve in the plane. Based on the obtained Pareto front, various LID designs and layouts can be selected according to actual needs and investment budgets. The key NSGA-II parameters followed the study of Yang et al. with a population size of 100, number of generations of 100, crossover probability of 0.8 and mutation probability as the reciprocal of the length [28].

3. Results

3.1. Global Convergence Evaluation of Optimization Model

The global convergence of the optimization model refers to its ability to converge the objective function values to a certain range as the number of generations increases. By observing the trend of the results for each generation, one can understand the overall change in the objective function values during the optimization process. In this study, the global convergence of the optimization model is assessed by observing the trend of the average values of the objective function results for each generation. When the average value of the objective function gradually stabilizes, it indicates that the optimization algorithm may be approaching a global optimum, as shown in Figure 9.

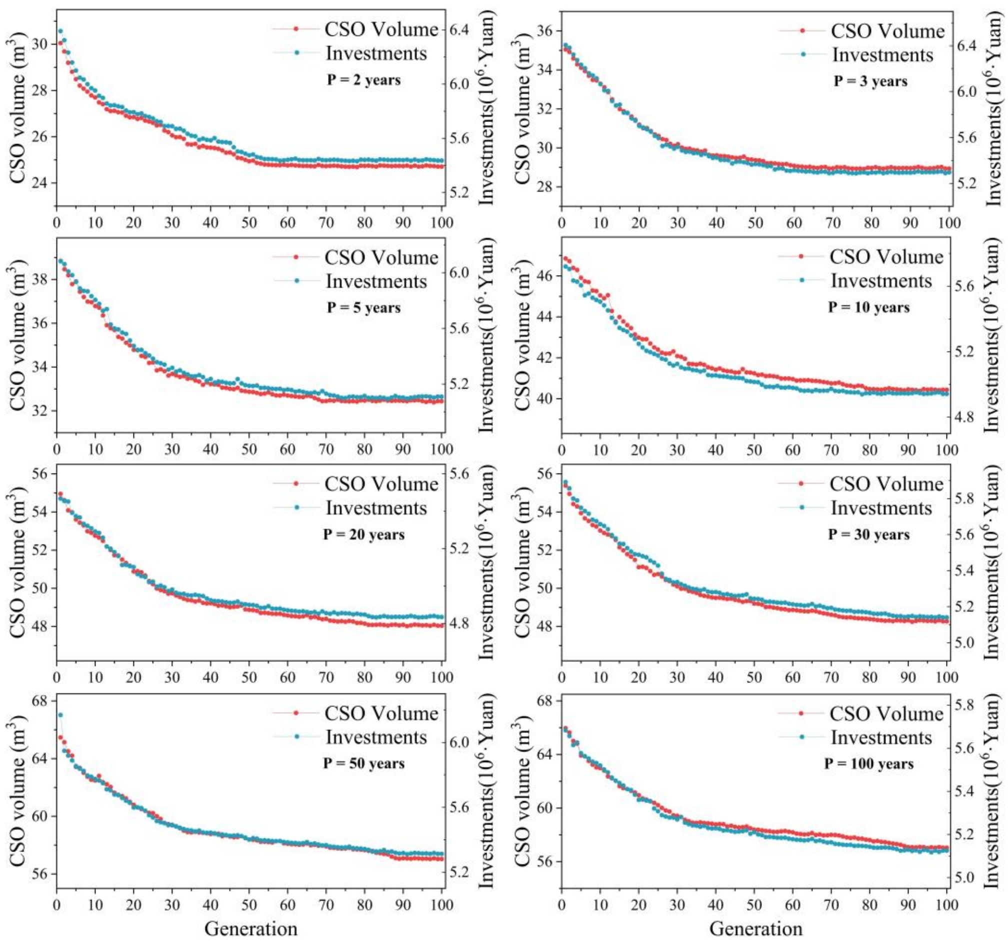

Figure 9. The mean values of the two objective functions for the eight different return periods.

In this optimization model, the total CSO overflow during a 2-year event begins to converge around the 55th generation, while the investment costs for construction and operation start to converge around the 60th generation. As the rainfall return period increases, the convergence generations of the model's average results gradually increase, from around 60 generations to about 90 generations. Typically, all objective function values converge after 90 generations, so setting the generation limit to 100 results in a converged optimization outcome. Once the model process terminates, the optimization results remain stable. This optimization model demonstrates good performance in assessing global convergence, providing stable optimization results and an effective method for addressing multi-objective optimization problems.

3.2. Pareto Frontier at Different Return Periods

The results of the Pareto frontier consisting of non-dominated solutions were obtained. As shown in Figure 10, the vertical axis represents the cost (in million RMB), and the horizontal axis represents the overflow volume (m^3). Each data point represents a solution, indicating the overflow volume of the combined sewer network for the corresponding scenario under given cost conditions. These data points are solutions obtained through non-dominated sorting from the last generation's merged population. After iterative optimization of the model under the 2-year design storm scenario, six dominant rank solutions were ultimately obtained. Among them, the points with Rank 0 form the Pareto frontier, while the other points are considered non-dominated solutions. It is observed that the Pareto frontier exhibits three different curve trends and discontinuities.

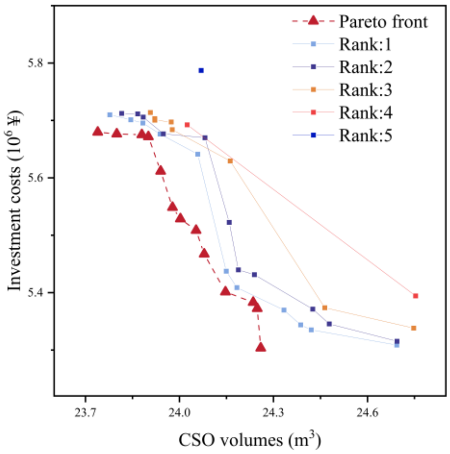

Figure 10. The Pareto front of the model under 2-year return period.

Under the current rainfall conditions, the solutions on the Pareto frontier show a range of variations in CSO overflow volume between 23.7 and 24.3 m^3 under different LID layout schemes, with total investment costs fluctuating between RMB 5.2 to 5.69 million. It can be observed that the CSO overflow volume and construction costs are approximately inversely proportional. Higher investment costs correspond to lower CSO volumes, and vice versa. In addition to the solutions on the Pareto frontier, there are also multiple non-dominated solutions. These non-dominated solutions are similar in shape to the Pareto frontier and are distributed outside it according to their rank. In practical applications, different design schemes can be selected according to planning requirements.

To compare the effects of different rainfall intensities on the optimization model and LID layout, this study obtained the optimized simulation results of eight LID layout methods in the study area under eight different return periods through the coupled model of SWMM and NSGA-II. As shown in Figure 11, the Pareto frontier of CSO overflow volume and investment cost is displayed. With the increase in the return period, the number of solution sets on the Pareto frontier gradually decreases. When the return period is 2 years, the maximum number of solution sets is 13, while when the return period is 100 years, the minimum number of solution sets is 5. There is no obvious trend in the shape of the Pareto solution set, and the curve is not monotonically decreasing, but exhibits a certain flat area and a steep area. In the flat area, the increase in cost has a smaller impact on reducing overflow volume, while in the steep area, even a slight change in cost will significantly reduce overflow volume.

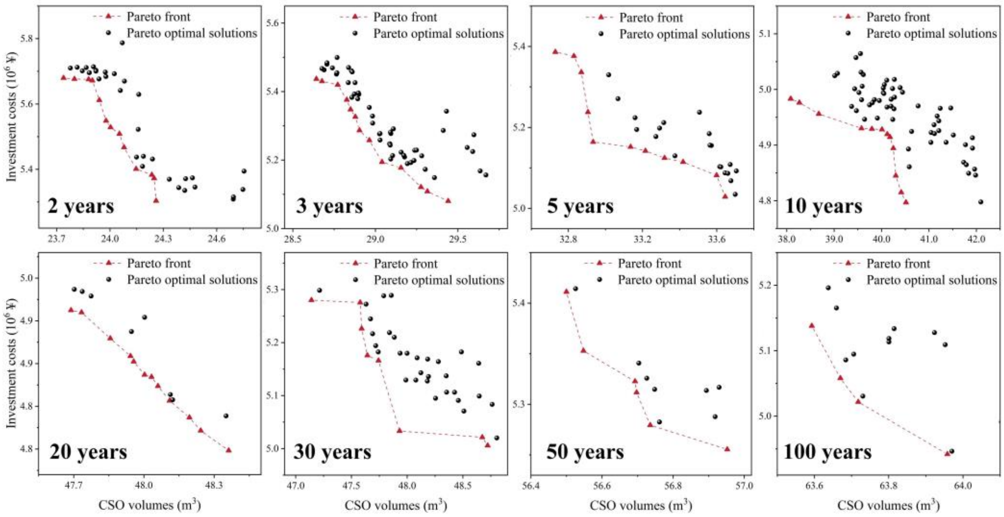

Figure 11. Pareto fronts of the model under different return periods.

By comparing these frontiers, it is observed that under the 2-year return period, the Pareto frontier of investment cost is the highest (Figure 12), ranging from 5.3 to 5.7 million. However, under the 20-year return period, the cost is the lowest, ranging from 4.72 to 4.91 million. With the increase in rainfall intensity, the total overflow volume continues to increase. The range of overflow volume corresponding to the Pareto frontier increases from 21–24.5 m^3 to 51–63 m^3, with an increase of about 147–159%. At the same time, the investment cost decreases from 5.3–5.7 billion to 4.92–5.13 million, with a decrease of 20.7–23.0%. Within the same construction cost range (RMB 5.3–5.38 million), the Pareto frontiers of the 2-year, 3-year, 5-year, and 50-year return periods intersect, so there may be an optimal layout scheme considering comprehensive factors. Meanwhile, as the rainfall return period increases, the slope of the Pareto frontier also increases gradually, from -7.2×10^5 to -5.4×10^5. This indicates that the LID control effect per unit cost is better at larger return periods. At the same time, it can be seen that the three trends of the Pareto frontier shown in Section 3.1 are more pronounced at lower return periods (P < 10 years), and as the return period increases, the differences between these three trends gradually disappear.

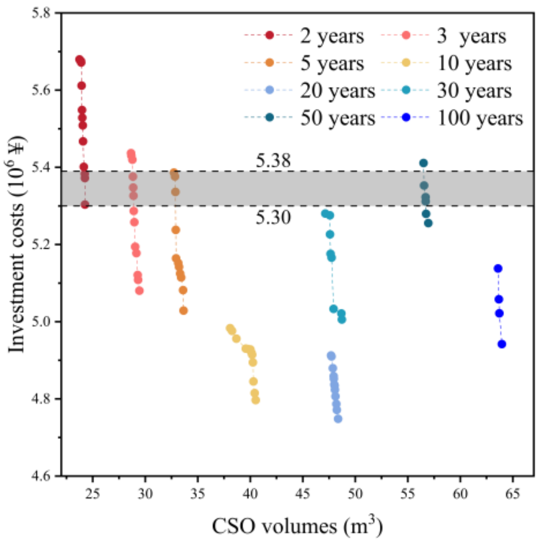

Figure 12. The Pareto front of the model under different rainfall return periods.

3.3. Optimal LID Variables of the Study Area

To further compare the impact of different rainfall intensities on the optimization model and LID layout, this study presents the optimization solutions and results for eight different return periods. The optimized simulation results of LID layout methods in the study area, obtained through the coupled model of SWMM and NSGA-II, serve as the basis for selecting the optimal layout scheme for the corresponding return period. Crowding distance, as a measure of solution distribution, can assist in selecting solutions with better diversity and balance. However, when choosing the optimal solution, other factors such as target weights, feasibility, etc., should also be considered. Only through a comprehensive consideration of these factors, balancing the actual research needs and decision-makers' preferences, can the optimal solution be selected. As shown in Figure 13, considering maximum crowding distance and highest unit cost-effectiveness (concave points) comprehensively, eight optimal solutions for different rainfall return periods were chosen.

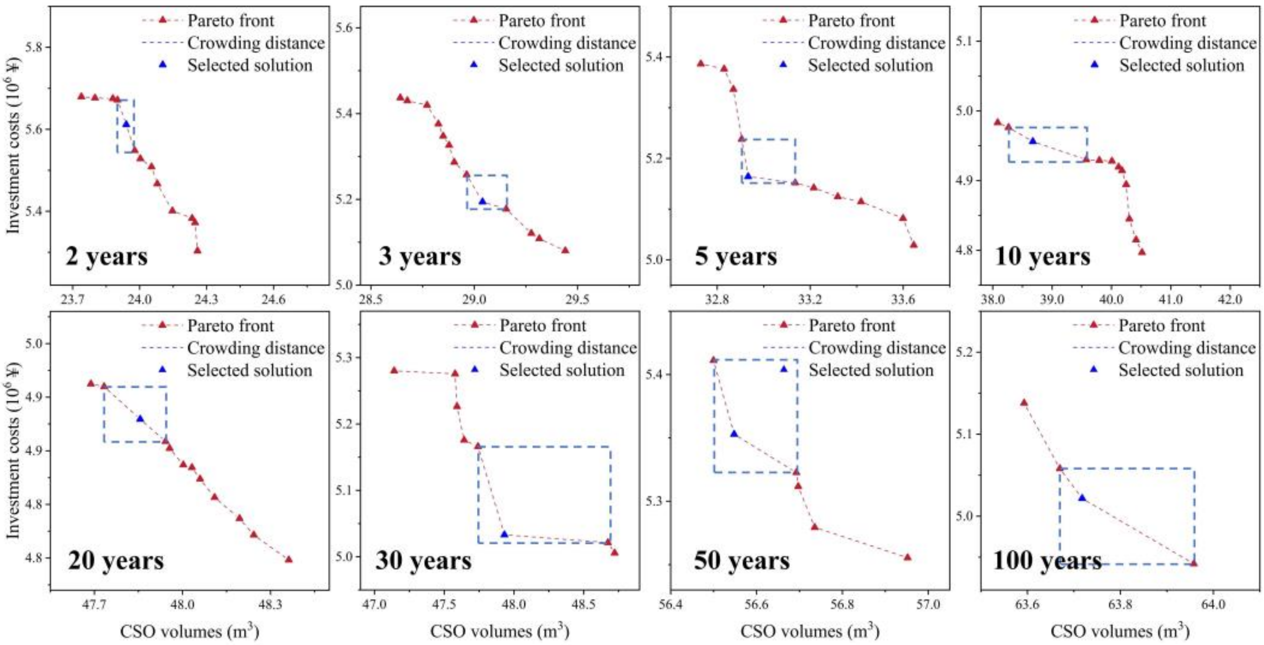

Figure 13. Optimal LID deployment scheme selection under different return periods.

The SWMM model was used to simulate CSO events under eight rainfall return periods, and the layout scales of three types of LID facilities were visualized. As shown in Figure 14, the optimal layout schemes for CSO overflow volume and investment cost considering eight different return periods are displayed. The research results indicate that the spatial distribution of LID layout is heterogeneous, with greater impacts in road and building-dense areas than in other areas. Under the eight return periods, 35.7% of LID locations have deployment proportions in the same range, while 87.3% of LID locations have deployment proportions in adjacent ranges (with deployment proportion differences less than 20%). These larger-scale deployment locations will be key spatial points to consider in LID planning and construction.

As the return period increases, as shown in Figure 15, the overall proportion of LID facilities in the optimal scheme generally shows a decreasing trend, while the CSO volume gradually increases. There is no apparent trend in the proportion of individual LID facilities. At the 3-year, 5-year, 20-year, and 30-year return periods, the proportion of permeable pavement in the optimal scheme is 38.4%; at the 3-year and 5-year return periods, the proportion of green roofs in the optimal scheme is 39.9%; at the 3-year and 5-year return periods, the proportion of rain gardens in the optimal scheme is 29.8%.

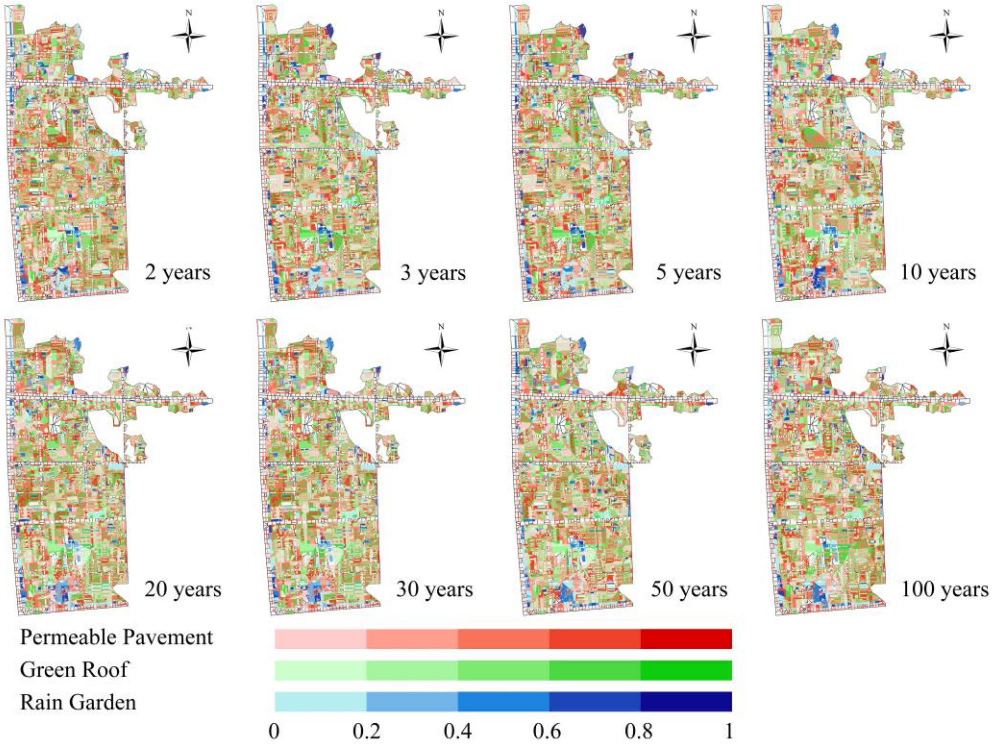

Figure 14. LID deployment scheme selection under different return periods.

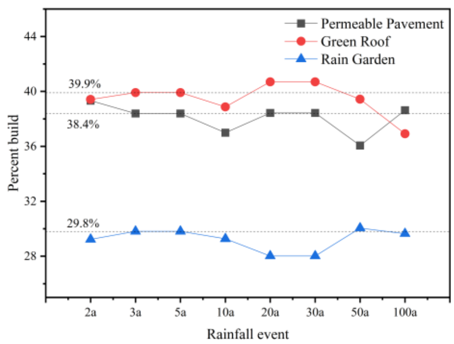

Figure 15. Optimal LID deployment proportion under different return periods.

4. Discussion

In terms of the simulation results of the optimization model for the 2-year return period, there are six levels of Pareto solution sets, with similar shapes and distribution patterns among different levels, presenting a curved distribution. As the cost increases, the overflow volume gradually decreases, reflecting the control effect of LID facilities on CSO and the performance of the optimization model. It is observed that on this Pareto frontier, three distinct trends emerge as the overflow volume increases. The first trend (AB) resembles a line with a slope of 0 degrees (Figure 10), indicating the existence of various layout schemes within this frontier where CSO control volume can be increased without significantly increasing the input cost. The second trend (BC) resembles a line or arc with a slope of 45 degrees (Figure 10), indicating the existence of various layout schemes within this trend where CSO control volume can be increased, but correspondingly, a certain construction cost is required. The third trend (CD) is more similar to a line with a slope approaching 90 degrees (Figure 10). Unlike the first trend, on this frontier, as the effectiveness of CSO control increases gradually with different schemes, the cost will sharply increase. It is generally believed that as investment increases, the improvement points in the system gradually decrease, and the remaining improvement space becomes more limited. This means that with each equal investment, the achievable runoff control rate will gradually decrease. When reaching a high level of investment, the return on investment will rapidly decrease. However, the sets of solutions on the Pareto frontier are contrary to this. In LID multi-objective optimization, the objective functions among different individuals are nonlinear. This means that within a certain range, increasing investment may result in nonlinear effects, leading to unconventional changes in returns.

As the rainfall intensity increases, the CSO constraints become more stringent. This finding indicates that higher rainfall intensity imposes greater demands on LID schemes to meet CSO control objectives. Consequently, the number of feasible solutions decreases, leading to a reduction in the quantity of Pareto frontier solution sets. Simultaneously, with the increase in rainfall intensity, there is a tendency for the Pareto frontier to move towards the lower left. This suggests an increase in CSO overflow volume, accompanied by a decrease in LID investment costs. This implies that achieving the same overflow control effect becomes more challenging at higher rainfall intensities by increasing the scale of LID construction. Additionally, LID facilities with higher investments are suitable for addressing CSO resulting from low-return period rainfall. However, blindly increasing the construction area and cost of LID to address high-return period rainfall may not be the optimal outcome.

According to Figure 11, the Pareto frontiers under different return periods do not intersect in terms of CSO volume. To determine a common solution for the eight return periods, the cost of LID is used as a constraint, and the boundaries of the feasible domain are defined. The minimum and maximum acceptable costs for LID construction are determined (as shown in the gray range). This helps to define the range of the feasible domain and exclude solutions that do not meet the constraints. By determining the boundaries of the feasible domain, the solution set can be restricted to the range of 5.3–5.38 million, filtering out solutions within the feasible domain. This means selecting solutions that comply with the constraint of LID construction cost. By confining the solution set within the feasible domain, the range of optimal solutions is narrowed, ensuring that the selected solution is the most appropriate one.

The chosen strategy of simultaneously considering maximum crowding distance and highest cost-effectiveness (concave points) resulted in the selection of eight optimal solutions for the different rainfall return periods. This approach ensures that the selected solutions have both good diversity and higher economic benefits. The selection of these optimal solutions for the eight return periods reflects a balance based on the comprehensive consideration of crowding distance and cost-effectiveness. These results provide valuable insights into the impact of varying rainfall intensities on the optimization model and LID layout strategies. The optimal LID layout results for the eight return periods offer crucial information regarding the spatial distribution and proportions of LID facilities. The heterogeneous spatial distribution indicates variations in the impact of LID layout across different areas, particularly in densely populated regions. This underscores the importance of considering local characteristics and focusing on areas with high returns and potential benefits. The variations in LID facility deployment proportions under different return periods demonstrate the adaptability of the optimal solutions to specific rainfall characteristics. The differences in deployment proportions reflect the trade-off between CSO control effectiveness and investment costs, highlighting the need to strike a balance between achieving the desired reduction in CSO and optimizing resource allocation.

The research results emphasize the importance of considering the spatial distribution and proportions of LID facilities in urban areas. Through visualizing the results, decision-makers can gain a deeper understanding of the optimal layout schemes under different return periods and prioritize areas that require immediate attention. This information can guide future planning and decision-making processes, effectively mitigating the impact of CSO events on densely populated and highly urbanized areas. In conclusion, the visualization of the optimal LID layout results for the eight return periods provides essential information about the spatial distribution and proportions of LID facilities.

5. Conclusions

This study is based on the NSGA-II multi-objective optimization algorithm and hydraulic network model to address CSO issues in the research area by optimizing LID layout schemes. Firstly, the SWMM model of the study area was constructed, and the types and scales of LID facilities were determined based on the land cover information of each sub-catchment. These details were then used as optimization variables passed to the SWMM model for hydrological process simulation and result retrieval. By iteratively solving through multi-objective optimization, the optimal Pareto frontier results were obtained. The main conclusions are as follows.

1. The stability of the optimization process and results of the coupled optimization model were first verified. The model, under designed storm scenarios, was able to obtain results of the Pareto frontier composed of non-dominated solutions. The results indicate that the solution sets obtained through Pareto frontier analysis exhibit different trends concerning cost-benefit. Under low costs, enhancing CSO control effectiveness of the optimal LID schemes requires a significant increase in construction costs; conversely, it is the opposite under high costs. There exists a nonlinear relationship between overflow volume and investment costs among different LID layout schemes, where increasing the scale of LID facilities does not necessarily imply a linear improvement in control effectiveness.
2. As rainfall intensity increases, the constraints on CSO become more stringent, resulting in a decrease in the number of feasible solutions and consequently reducing the quantity of Pareto frontier solution sets. Additionally, achieving the same overflow control effect by increasing the scale of LID construction becomes more challenging under higher rainfall intensities. LID facilities with higher investments are suitable for addressing CSO issues caused by low-return period rainfall, but blindly increasing the construction area and cost of LID may not be the optimal layout solution for high-return period rainfall. When considering the eight return periods, narrowing down the selection range by using construction costs within the range of 5.3–5.38 million as a constraint can help find the most suitable layout scheme.
3. By considering the balance between maximum crowding distance and highest cost-effectiveness, eight optimal solutions were selected for different rainfall return periods. This approach ensures that the chosen solutions have diversity and higher economic benefits. The selection range was determined for key LID layout points and their scales in the research area, achieving a proportion of 35.7%. The variations in the proportion of LID facility deployment under different return periods reflect the trade-off relationship between CSO control effectiveness and investment costs.
4. The results of this study aim to construct a coupled model and identify the relationship between LID layout schemes, investment costs, and combined sewer network overflow, particularly LID layout schemes under different rainfall return periods. These provide urban drainage departments with LID solutions to address overflow risks under various rainfall return periods, thereby enhancing the operational planning level of drainage management departments during rainy days. Additionally, quantitative comparisons were made regarding the distribution of LID layout points and construction proportions under the eight optimal layout schemes, enabling the precise identification of potential optimal LID layout points when rainfall occurs. This allows drainage management departments to better address overflow risks in combined sewer networks during rainy days.

Author Contributions: Conceptualization, P.Z. and H.W.; methodology, H.W. and J.Z.; software, P.Z. and H.W.; validation, Z.L.; formal analysis, P.Z. and J.Z; data curation, W.L.; writing—original draft preparation, P.Z.; writing—review and editing, P.Z.; supervision, W.L. All authors have read and agreed to the published version of the manuscript.

Funding: This research was funded by the R&D Program of Beijing Municipal Education Commission (grant number: KM202210005017), Major Science and Technology Innovation Pilot Project for Water Resources Protection and Integrated-Saving Utilization in the Yellow River Basin of Inner Mongolia Autonomous Region (grant number: 2023JBGS0007), National Natural Science Foundation of China General Project (grant number: 72373011), Beijing Natural Science Foundation (grant number: 8242003), and R&D Program of Beijing Municipal Education Commission (grant number: KM202310005023).

Data Availability Statement: The data presented in this study are available on request from the corresponding author.

Conflicts of Interest: Author Zilong Liu was employed by the company Beijing Municipal Institute of City Planning and Design. Author Wentao Li was employed by the company Guangzhou Municipal Engineering Design & Research Institute Co., Ltd. The remaining authors declare that the research was conducted in the absence of any commercial or financial relationships that could be construed as a potential conflict of interest.

References

1. Bertels, D.; De Meester, J.; Dirckx, G.; Willems, P. Estimation of the impact of combined sewer overflows on surface water quality in a sparsely monitored area. *Water Res.* **2023**, *244*, 120498. [CrossRef] [PubMed]
2. Matsui, K.; Miki, T. Microbial community composition and function in an urban waterway with combined sewer overflows before and after implementation of a stormwater storage pipe. *PeerJ* **2023**, *11*, e14684. [CrossRef] [PubMed]
3. Riechel, M.; Matzinger, A.; Pallasch, M.; Joswig, K.; Pawlowsky-Reusing, E.; Hinkelmann, R.; Rouault, P. Sustainable urban drainage systems in established city developments: Modelling the potential for CSO reduction and river impact mitigation. *J. Environ. Manag.* **2020**, *274*, 111207. [CrossRef] [PubMed]
4. Saddiqi, M.M.; Zhao, W.; Cotterill, S.; Dereli, R.K. Smart management of combined sewer overflows: From an ancient technology to artificial intelligence. *Wiley Interdiscip. Rev.-Water* **2023**, *10*, e1635. [CrossRef]
5. Jean, M.È.; Morin, C.; Duchesne, S.; Pelletier, G.; Pleau, M. Optimization of real-time control with green and gray infrastructure design for a cost-effective mitigation of combined sewer overflows. *Water Resour. Res.* **2021**, *57*, e2021WR030282. [CrossRef]
6. Quaranta, E.; Fuchs, S.; Liefting, H.J.; Schellart, A.; Pistocchi, A. Costs and benefits of combined sewer overflow management strategies at the European scale. *J. Environ. Manag.* **2022**, *318*, 115629. [CrossRef] [PubMed]
7. Liu, T.; Lawluvy, Y.; Shi, Y.; Yap, P. Low Impact Development (LID) Practices: A review on recent developments, challenges and prospects. *Water Air Soil Pollut.* **2021**, *232*, 344. [CrossRef]
8. Li, C.; Zhang, Y.; Wang, C.; Shen, R.; Gisen, J.; Mu, J. Stormwater and flood simulation of sponge city and LID mitigation benefit assessment. *Environ. Sci. Pollut. Res.* **2023**, *30*, 1–17. [CrossRef] [PubMed]
9. Liu, Z.; Li, W.; Wang, L.; Li, L.; Xu, B. The scenario simulations and several problems of the sponge city construction in semi-arid loess region, Northwest China. *Landsc. Ecol. Eng.* **2022**, *18*, 95–108. [CrossRef]
10. Gong, Y.; Chen, Y.; Yu, L.; Li, J.; Pan, X.; Shen, Z.; Xu, X.; Qiu, Q. Effectiveness analysis of systematic combined sewer overflow control schemes in the Sponge City pilot area of Beijing. *Int. J. Environ. Res. Public Health.* **2019**, *16*, 1503. [CrossRef] [PubMed]
11. Liu, Y.; Ahiablame, L.M.; Bralts, V.F.; Engel, B.A. Enhancing a rainfall-runoff model to assess the impacts of BMPs and LID practices on storm runoff. *J. Environ. Manag.* **2015**, *147*, 12–23. [CrossRef] [PubMed]
12. Gao, J.; Li, J.; Li, Y.; Xia, J.; Lv, P. A distribution optimization method of typical LID facilities for Sponge City construction. *Ecohydrol. Hydrobiol.* **2021**, *21*, 13–22. [CrossRef]
13. Zeng, J.; Huang, G.; Mai, Y.; Chen, W. Optimizing the cost-effectiveness of low impact development (LID) practices using an analytical probabilistic approach. *Urban Water J.* **2020**, *17*, 136–143. [CrossRef]
14. Liao, Z.L.; Zhang, G.Q.; Wu, Z.H.; He, Y.; Chen, H. Combined sewer overflow control with LID based on SWMM: An example in Shanghai, China. *Water Sci. Technol.* **2015**, *71*, 1136–1142. [CrossRef] [PubMed]
15. Yao, L.; Wu, Z.; Wang, Y.; Sun, S.; Wei, W.; Xu, Y. Does the spatial location of green roofs affects runoff mitigation in small urbanized catchments? *J. Environ. Manag.* **2020**, *268*, 110707. [CrossRef]
16. Tansar, H.; Duan, H.; Mark, O. Catchment-scale and local-scale based evaluation of LID effectiveness on urban drainage system performance. *Water Resour. Manag.* **2022**, *36*, 507–526. [CrossRef]
17. Cheng, X.; Wang, H.; Chen, B.; Li, Z.; Zhou, J. Comparative analysis of flood prevention and control at LID facilities with runoff and flooding as control objectives based on InfoWorks ICM. *Water* **2024**, *16*, 374. [CrossRef]
18. Saniei, K.; Yazdi, J.; Majdzadeh Tabatabei, M.R. Optimal size type and location of low impact developments LIDs for urban stormwater control. *Urban Water J.* **2021**, *18*, 585–597. [CrossRef]
19. Ambrogi Ferreira Do Lago, C.; Shahrokh Hamedani, A.; Mendiondo, E.M.; Hofheinz Giacomoni, M. Simulation and optimization framework for evaluating the robustness of low-impact development placement solutions under climate change in a small urban catchment. *Hydrolog. Sci. J.* **2023**, *68*, 2057–2074. [CrossRef]
20. Yu, Y.; Zhou, Y.; Guo, Z.; van Duin, B.; Zhang, W. A new LID spatial allocation optimization system at neighborhood scale: Integrated SWMM with PICEA-g using MATLAB as the platform. *Sci. Total Environ.* **2022**, *831*, 154843. [CrossRef]

21. Liu, K.; Chen, B.; Wang, S.; Wang, H. An urban waterlogging footprint accounting based on emergy: A case study of Beijing. *Appl. Energy* **2023**, *348*, 121527. [CrossRef]
22. Dong, Z.; Bain, D.J.; Akcakaya, M.; Ng, C.A. Evaluating the Thiessen polygon approach for efficient parameterization of urban stormwater models. *Environ. Sci. Pollut. Res.* **2023**, *30*, 30295–30307. [CrossRef] [PubMed]
23. *DB11/T2074-2022*; Technical Specification for Construction and Application of Mathematical Model of Urban Flooding Prevention and Control System. Beijing Municipal Commission of Planning and Natural Resources, Beijing Municipal Bureau of Market Supervision and Administration: Beijing, China, 2022.
24. Mishra, G.; Ghosh, K.; Dwivedi, A.K.; Kumar, M.; Kumar, S.; Chintalapati, S.; Tripathi, S.N. An application of probability density function for the analysis of PM2.5 concentration during the COVID-19 lockdown period. *Sci. Total Environ.* **2021**, *782*, 146681. [CrossRef] [PubMed]
25. Zhou, J.; Pang, Y.; Wang, H.; Li, W.; Liu, J.; Luo, Z.; Shao, W.; Zhang, H. Sewage network operational risks based on InfoWorks ICM with nodal flow diurnal patterns under NPIs for COVID-19. *Water Res.* **2023**, *246*, 120708. [CrossRef] [PubMed]
26. *DB11/T 1743-2020*; Standard for Sponge City of Construction and Design. Beijing Municipal Commission of Planning and Natural Resources, Beijing Municipal Bureau of Market Supervision and Administration: Beijing, China, 2021.
27. *Sponge City Construction Technical Guide*; Ministry of Housing and Urban-Rural Development of the People's Republic of China: Beijing, China, 2014.
28. Yang, B.; Zhang, T.; Li, J.; Feng, P.; Miao, Y. Optimal designs of LID based on LID experiments and SWMM for a small-scale community in Tianjin, north China. *J. Environ. Manag.* **2023**, *334*, 117442. [CrossRef] [PubMed]